19th Australasian Fluid Mechanics Conference
Melbourne, Australia
8-11 December 2014

Momentum and Vorticity Balances in a Jet that Issues from a Sharp-edged Rectangular Orifice

A. P. Vouros[1], A. Pollard[2], T. Panidis[1] and R.Schwab[2]

[1]Mechanical Engineering and Aeronautics Department, University of Patras, 26504 Patras, Greece

[2]Department of Mechanical and Materials Engineering, Queen's University at Kingston K7L-3N6, Ontario, Canada

Abstract

Experimental results on the near field development of a free rectangular jet with aspect ratio 10 are presented. The jet issues from a sharp-edged orifice attached to a rectangular settling chamber at $Re_{D_h} \approx 42{,}000$. Measurements on cross plane grids were obtained with a two-component hot-wire anemometry probe, which provided information on the three dimensional characteristics of the flow field. Two key features of this type of jet are saddleback mean axial velocity profiles and a predominant dumbbell shape as described by, for example, a contour of the axial mean velocity. The saddleback shape is found to be significantly influenced by the vorticity distribution in the transverse plane of the jet, while the dumbbell is traced to two terms in the axial mean vorticity transport equation that diffuse fluid from the centre of the jet towards its periphery

Introduction

Rectangular jets have been studied extensively as a fundamental problem in turbulence and as a generic flow configuration in engineering applications. In the past, studies focused on the effect of a wide variety of initial-boundary conditions, which affect the development and the characteristics of the mean and turbulent properties of the jet.

Based on previous experimental work that demonstrated that axial mean velocity profiles featured a saddle-backed shape for aspect ratios AR$\geq$ 5, Tsuchiya *et al.* (1986) presented profiles of the velocity and temperature fields, and discussed the source of their formation in relation to the mixing process in the two directions perpendicular to the jet streamwise axis. They discussed extensively the spreading characteristics of three jets issuing from different nozzles (smoothed, orifice and long pipe) and concluded that except for the different geometry, the jet Reynolds number and also the low aspect ratios can produce remarkable changes on jet half-width and the downstream evolution of the turbulence intensity of the streamwise velocity. Quinn *et al.* (1985) and Quinn and Militzer (1988) studied extensively the development of rectangular jets, and presented velocity and pressure measurements along with numerical simulations of the mean and turbulent statistics. They also confirmed that saddle-backed profiles are formed for aspect ratio greater than a value of about five. Based on the axial evolution of the streamwise velocity, they discussed the more efficient mixing with the surrounding air of rectangular compared to axisymmetric jets. Pollard and Iwaniw (1985) and Schwab (1986) used rectangular jets with and without corner rounding and found saddle-backed profiles in both cases. Schwab (1986) was the first to obtain, but did not fully interpret, cross-plane data so as to assess the three-dimensional features of the flow development. Additional studies were presented by Quinn (1991, 1992) and Grandmaison *et al.* (1991) with the latter reporting on the characteristics of the mixing of passive scalars in rectangular jets with high and small aspect ratio, respectively, while Quinn (1995) and Lozanova and Stankov (1998) discussed the mean and turbulence properties, the entrainment and the mixing process of jets issuing from contoured and smooth contraction rectangular jets with several aspect ratios. It is important to note that Quinn (1992) in his study of effects of jet aspect ratio, the orifices were attached to a settling chamber that was square in cross section (as were the experiments of Schwab, Iwaniw and Pollard and Quinn *et al.*); thus, the flow entering the orifice from the chamber does so with streamline curvature that is different in the y and z planes; thus, for small aspect ratios no saddle backed velocity profiles were noted, which implies minimum sensitivity to that difference in curvature, whereas these saddle shapes in the axial mean velocity increased significantly with increasing aspect ratio. The sensitivity to jet aspect ratio was amply displayed in the triple velocity correlations, Quinn (1992) .

During the last decade, the University of Adelaide group (Mi *et al.* 2005, Deo *et al.* 2007a, 2007b, 2008) conducted a systematic investigation in order to distinguish the features that arise from different Reynolds numbers, the aspect ratio and the geometrical characteristics of smoothed-edged nozzles. They discussed extensively the various trends observed in the axial velocity decay, the jet half-width and the mean and turbulent velocity profiles on the main axis of symmetry of the flow, which are closely related to the initial boundary layer displacement and momentum thickness. They showed that saddle-backed profiles maybe eliminated by increasing the radius of the smoothed part of the orifice at the exit. Alnahhal and Panidis (2009) and Alnahhal *et al.* (2011) conducted experiments in order to reveal the effects of both end-plates and sidewalls on the streamwise evolution and the cross plane profiles of the mean and turbulent components. Results were discussed with respect to the interplay of the dominant mechanisms at the exit plane of the jet, which include the shear layer development at the short-side edges.

Computationally, Wilson and Demuren (1998) used large eddy simulation, with a Smagorinsky sub-grid model. At low Re (=750), where LES was not invoked, axis switching "is based on self-induction of the vorticity field", whereas for Re=75,000 they argue it is the anisotropy in the Reynolds stresses that dominates since at these higher Re, the broad spectrum of instabilities in the shear layers precludes self induction. Grinstein (1995) also used LES to investigate vortex ring evolution from low-aspect ratio rectangular jets. To the authors' knowledge, these calculations were the first to identify and rather convincingly explain the vortex formation and their spatial and temporal evolution.

Tipnis (2009) and Tipnis *et al.* (2013) considered the effects of upstream conditioning of the flow on the formation of streamwise vorticity. They used LDV and commercial CFD and RANS and captured axial vorticity that appears in favourable accord with data of Zaman (1996) even though earlier work argued (Wilson and Demuren 1998) that isotropic models are inappropriate. The upstream contractions all smoothly lead into the rectangular nozzles, as opposed to the use of an orifice plate (see Quinn *et al.* 1985)

More recently, Yu and Girimaji (2005, 2006, 2008) and Chen

and Yu (2014) considered rectangular jets through the application of the lattice Boltzmann method as an alternate vehicle for LES to simulate the flow from low aspect ratio rectangular jets. They noted the importance of the jet corner axial vorticity and the role it plays to deform the jet (axis switching); they also featured "puffs" and a general dumbbell cross-sectional shape (see figure 21 of Yu and Girimaji, 2005); however, as will be argued here, their explanation for the appearance of the saddle-backed velocity profiles is not convincing.

From the above, a critical feature of rectangular jet flows from an orifice is the formation of saddle backed velocity profiles. The present work uses the data from Schwab (1986) who performed measurements to obtain mean and Reynolds stresses on the central axis of jets and on a variety of cross-plane layers with respect to the streamwise axis, but only to x/h=30, which is at the onset of axis switching. Those data are further analyzed here by carefully interpolating these data to produce maps of streamwise vorticity as well as analyzing the relative importance of terms in the axial mean vorticity and momentum equations to monitor the initial formation and downstream evolution of saddle-backed velocity profiles.

Experimental Conditions

The jet was produced by a sharp-edged rectangular orifice of dimensions 70×7 mm^2 (equivalent hydraulic diameter $D_h =$ 12.73 mm) mounted on the downsaatream end of a square cross sectioned settling chamber 0.350 m to the side. A small blower was used to supply air through the settling chamber, while flow straightening devices, including a baffle, filter material, honeycomb and screens, were used to reduce the turbulence levels in the flow. The exit Reynolds number based on the slot height ($h = 7$ mm) was approximately 23,000 or approximately Re_{D_h} = 42,000 based upon the hydraulic diameter; therefore, the exit velocity, $U_{exit} \approx 50\ m/s$.

A double layer of wire mesh screens surrounded the jet flow thereby minimising influence from external disturbances. Measurements were carried out using an X hot-wire probe. The velocity components in the streamwise (x-axis) and the spanwise (y-axis) directions were measured and upon probe rotation the lateral velocity components were obtained (z-axis). Data were collected on a cross plane grid at 40 by 16 equally spaced positions, at x/h= 0, 1, 2, 5, 10 and 30. These data were then subjected to careful interpolation, see Vouros *et al.* (2014). In the central area of the jet, the estimated uncertainties were 1% in the measured mean velocities, 6% in the fluctuating (rms), 6% in the Reynolds stresses and 5% positioning error for the yaw and pitch angles of $\pm 12^o$. At the jet edges and especially close to the exit, the presence of steep gradients or very low streamwise velocities may lead to significantly higher uncertainties. The origin of the Cartesian coordinate system used in this work is located at the centre of the orifice on the jet exit plane. The x axis points downstream in the streamwise direction, whereas the y and z axes are in the spanwise and lateral direction along the long and short sides of the nozzle, respectively.

Presentation and Discussion of Results

The data have been imported into Tecplot^{TM} and the various terms have been calculated in the axial mean momentum and the axial mean vorticity equation. These equations are not reproduced here for space considerations; however, a reader may refer to Launder and Rodi (1983) as we will use the same nomenclature here.

Axial Mean Momentum

Iso-contours of the convection and Reynolds stress terms in the axial mean momentum equation, suitably normalised by U_{cl} are presented in figure 1 and 2. There are 7 planes presented for x/h=0, 1, 2, 5, 7, 10 and 13 and the magnitude of the terms in each cross plane are equally scaled. In all cases there is excellent symmetry in the distributions of these quantities. The black contour line in each figure represents $U/U_{cl} = 0.5$ and at locations intermediate to $x/h = 0\&13$ and feature the "puffs" referred to by Yu and Girimaji; in fact flow visualization in the current study also clearly identified these features.

The additional two terms in the momentum equation (pressure gradient and diffusion) make up the slight difference between the two terms presented and, for example, as presented in figure 3, along the central span wise direction at $x/h = 10$ the magnitude of these terms sum to about 0.01 or about 10% of the $\pm$ scale of the plots. The separation in magnitude of the convection and Reynolds stress terms towards the outer portions of the jet at $x/h = 10$ indicate their competing influence. It is interesting to note that the balance in these terms is markedly different to those presented by Wilson and Demuren (1998) in that their simulation data indicated very little change at the jet edges but significant differences in the central portion of their jet. This could be due to their use of a 2:1 aspect ratio rather than 10:1 aspect ratio jet used here, which suggests that further work is required to explore these features as a function of both aspect ratio and nozzle configuration as used by Tipnis *et al.* (2013).

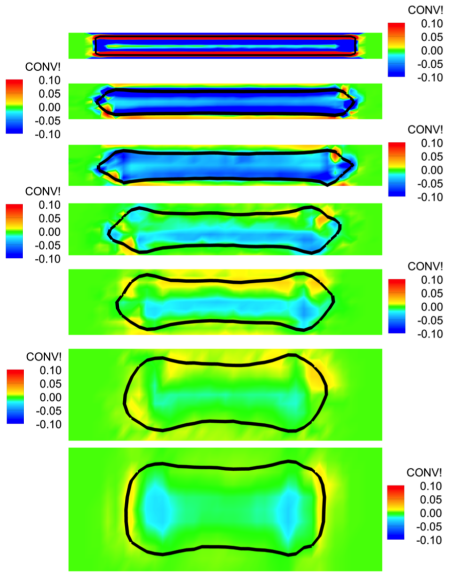

Figure 1: Mean axial momentum convection term distributions in transverse plane x/h=0, 1, 2, 5, 7, 10 and 13 (top to bottom)

Vorticity Characteristics and the Saddled-backed Velocity Profile

The vorticity magnitude normalised using U_{exit}/h, $|\Omega|$, is first presented in figure 4. The plot displays contours at x/h=0, 1, 2,5, 10 and 30. Please note $0 \leq |\Omega| \leq 2.0$ is the vorticity magnitude scale. At x/h=0 the flow seems to be dominated by the streamwise velocity shear layers. Peak values are aligned with the $U/U_{cl} = 0.5$ boundary (the black outline) in the near field. At $x/h = 10$ the short side shear layers result in higher total vorticity magnitude values, which is a feature that persists even at $x/h = 30$ despite the "axisymmetry" of the flow field.

Each of the five terms in the axial mean vorticity equation (see Launder and Rodi 1983) has been calculated for $0 \leq x/h \leq 13$ and terms B ($\Omega_Y \frac{\partial U}{\partial y}$) and C ($\Omega_Z \frac{\partial U}{\partial z}$), which reflect the streamwise velocity distribution, are presented in figures 5 and 6.

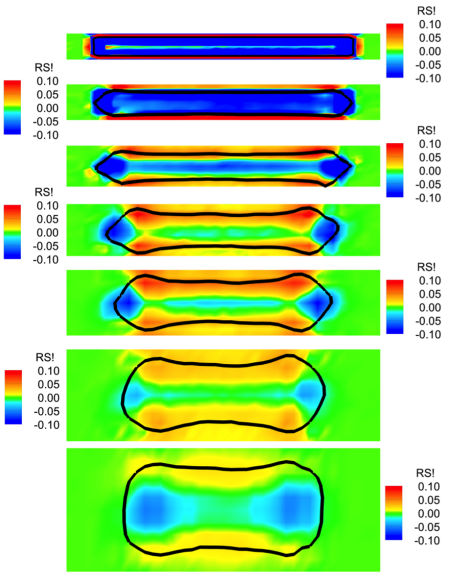

Figure 2: Mean axial momentum total Reynolds stress term distributions in transverse plane x/h=0, 1, 2, 5, 7, 10 and 13 (top to bottom)

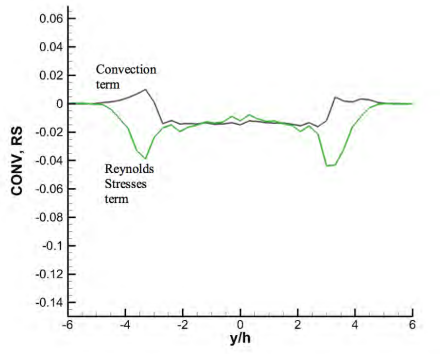

Figure 3: Distribution of the mean axial momentum total Reynolds stress and convection terms in transverse plane x/h=10.

Please note the difference in the scales as x/h is increased. Attention is first directed to the plots at $x/h = 0$ where is it noticed the symmetry in the contours and the magnitude (± 0.5) of the values. It must be remarked that all other terms in the vorticity transport equation are of similar magnitude as for those terms, except for the dissipation, determined by balance, which are very small. Immediately, it is noticed that with distance downstream, the deformation of the mean velocity curve follows the sense of rotation indicated. Consider the top right corner in the figure where $\Omega_Y \frac{\partial U}{\partial y}$ is positive (red) and $\Omega_Z \frac{\partial U}{\partial z}$ is negative (blue). This implies that these terms are responsible for drawing fluid towards and away from the jet centreline to give rise to part of the dumbbell shape, while term C (Ω_Z) is responsible for stretching the shape outward thereby completing the dumbbell shape. For interest, all other terms in the equation, including term A, decrease in magnitude relative to terms B and C so that by $x/h = 10$, say, they are all an order of magnitude smaller than terms B and C. The question now arises if terms B and C contribute to the formation of the saddle backed velocity profiles. It is to be recalled that it is at $x/h \sim 10$ where the saddle-backed velocity profiles are very apparent. The answer is not clear. Certainly the intersection of the positive and negative regions of terms B and C in the axial vorticity equation are again precisely centred at the location of the saddleback peaks; however, the orientation of Ω_Y and Ω_Z vectors suggest removal of fluid from the peak region and moreover the magnitudes of these terms is significantly below those of the mean vorticity. Therefore, all that maybe said is that terms B and C assist to diffuse high velocity fluid away from the peak region thereby lowering its magnitude from what it would attain in their absence. As a result, there emerges with distance downstream of the orifice, the saddle-backed velocity profiles.

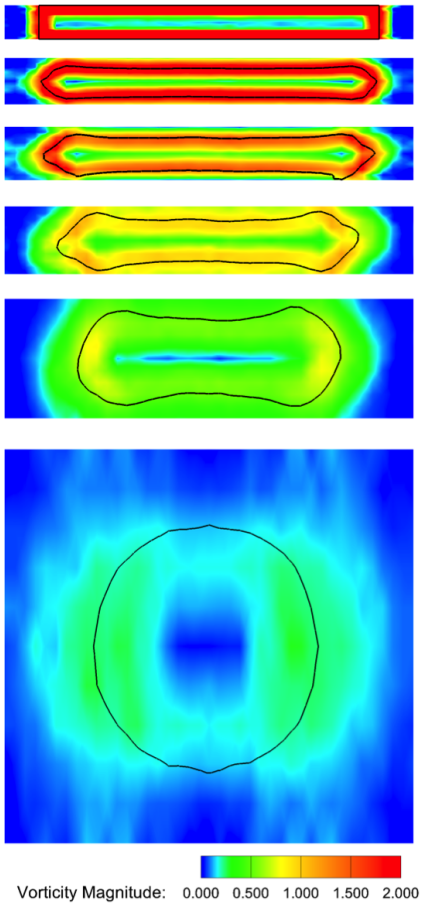

Figure 4: Contours of the magnitude of the vorticity vector at x/h =0, 1, 2, 5, 10 and 30.

Conclusion

From the current contribution, it can be concluded that the rectangular jet considered here is substantially no different to what other experiments have revealed; however, from the examination of the vorticity field and the mean axial vorticity equation, the saddleback velocity profiles are a result of transverse vorticity; moreover, the general evolution of the cross sectional shape of the jet appears to a result of corner vortices at the beginning of the jet that eventually distort the cross-section of it from rectangular to a dumbbell shape and the intersection of spanwise and transverse axial vorticity fluxes, $\Omega_Y \frac{\partial U}{\partial y}$) and ($\Omega_Z \frac{\partial U}{\partial z}$, which coincide with the location of the saddleback velocity profiles.

Acknowledgements

This work was supported by grants from NSERC (Canada), The University of Patras and Queen's University. This work emerged from a sabbatical visit by AP to University of Patras.

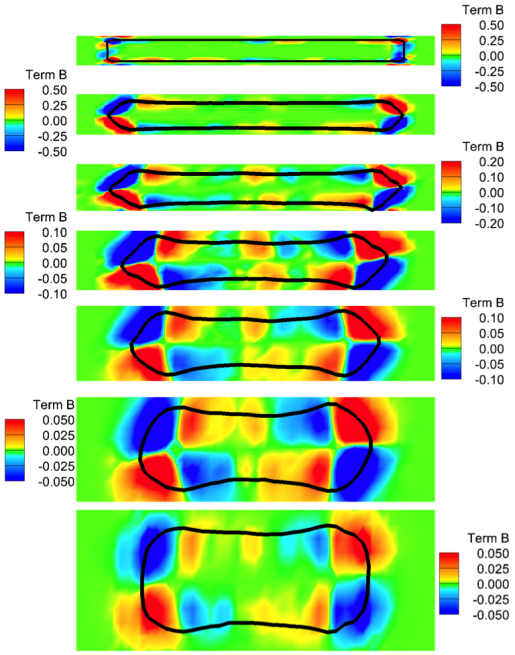

Figure 5: Term B ($\Omega_Y \frac{\partial U}{\partial y}$) in mean axial vorticity eqn. x/h=0, 1, 2, 5, 7, 10 and 13 [top to bottom].

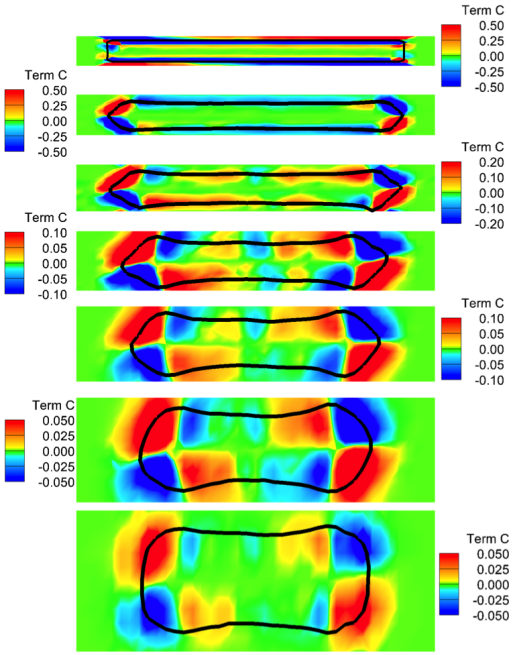

Figure 6: Term C ($\Omega_Z \frac{\partial U}{\partial z}$) in mean axial vorticity eqn. x/h=0, 1, 2, 5, 7, 10 and 13 [top to bottom].

References

References

[1] Alnahhal, M., Cavo, A., Romeos, A., Perrakis, K., Panidis, T., 2011. Eur. J. Mech./B Fluids 30, 451-465.

[2] Alnahhal, M., Panidis, Th., 2009. Exp. Therm. Fluid Sci. 33, 838-851.

[3] Deo, R. C., Mi, J., Nathan G. J., 2007a. Exp.Therm. Fluid Sci. 32, 545-559.

[4] Deo, R. C., Mi, J., Nathan G. J., 2007b. Exp.Therm. Fluid Sci. 31, 825-838.

[5] Deo, R. C., Mi, J., Nathan G. J., 2008. Phys. Fluids 20, 075108.

[6] Grandmaison, E. W., Pollard, A., Ng, S., 1991. Int. J. Heat Mass Trans. 34, 2653-2662.

[7] Grinstein, F., 1995 Phys. Fluids, 7(10):2519-2521.

[8] Grinstein, F., 2001. J. Fluid Mech. 437, 69-101

[9] Launder, B.E., Rodi, W. 1983. Ann. Rev. Fluid Mechanics, 15:429-459

[10] Lozanova, M., Stankov, P., 1998. . Exp. Fluids 24, 470-478.

[11] Mi, J., Deo, R. C., Nathan, G. J., 2005. Phys. Fluids 17, 068102.

[12] Pollard, A., Iwaniw, M. A., 1985. AIAA J. 23, 631-633.

[13] Quinn, W., 1991. AIAA J. 29, 515-519

[14] Quinn, W. R. 1992, Expt. Thermal Fluid Science, 5, 203-215.

[15] Quinn, W., 1995. Aeron. J. 99, 337-342.

[16] Quinn, W. R., Militzer, J., 1988. Phys. Fluids 31, 1017-1025.

[17] Quinn, W. R., Pollard, A., Masters, G. F., 1985. AIAA J. 23, 971-973.

[18] Schwab, R.R., 1986. Ph.D. Thesis, Department of Mechanical Engineering, Queen's University.

[19] Tipnis, T.J. 2009. Ph.D. Thesis, Cranfield University.

[20] Tipnis, T.J., Knowles, K., Bray, D. 2013. Proceedings of the Institution of Mechanical Engineers, Part G: Journal of Aerospace Engineering, 227(8): 1325-1337

[21] Tsuchiya, Y., Horikoshi, C., Sato T., 1986. Exp. Fluids 4, 197-204.

[22] Wilson, R., Demuren, A.O., 1998. ASME J. Fluids Engg. 120:285-290.

[23] Yu, H., Girimaji, S., 2005. Phys. Fluids, 17, 125106 (2005); doi: 10.1063/1.2140021

[24] Yu, H., Girimaji, S., 2006. Physica A, 362, 151-157

[25] Yu, H., Girimaji, S., 2008. 55, 1611-1619

[26] Zaman, K. B. M. Q., 1996. J. Fluid Mech. 316, 1-27